Epigallocatechin-3-gallate affects the proliferation, apoptosis, migration and invasion of tongue squamous cell carcinoma through the hippo-TAZ signaling pathway

AONAN LI[1,2], KE GU[1,2], QI WANG[1,2], XIYAN CHEN[1,2], XUCHENG FU[1,2], YING WANG[1,2] and YONG WEN[1,2]

[1]Department of Implantology, School of Stomatology, Shandong University, Jinan, Shandong 250012;
[2]Shandong Provincial Key Laboratory of Oral Tissue Regeneration, Department of Implantology,
Jinan, Shandong 250100, P.R. China

Abstract. The purpose of the present study was to investigate the mechanism by which epigallocatechin-3-gallate (EGCG) inhibits the biological behaviors of the tongue squamous cell carcinoma (TSCC) through the Hippo-tafazzin (TAZ) signaling pathway and to provide insights into molecular targeted therapy in TSCC. CAL27 and SCC15 cells were treated with different concentrations of EGCG for 24 h. Cell proliferation was determined using Cell-Counting Kit-8 and EdU assays. Cell apoptosis was evaluated by flow cytometry. Cell migration and invasion were measured using scratch and Transwell assays, respectively. Furthermore, protein levels of associated target genes were detected using a western blot assay. It was demonstrated that EGCG affected biological behaviors of CAL27 and SCC15 cells in concentration- and time-dependent manners. In addition, EGCG decreased the protein levels of TAZ, LATS1, MOB1 and JNK. Overexpression of TAZ alleviated the effect of EGCG on CAL27 cells. Furthermore, the combination of EGCG and simvastatin inhibited the proliferation, migration and invasion, and promoted apoptosis significantly compared with single treatment in CAL27 cells. The results of the present study suggested that EGCG affects proliferation, apoptosis, migration and invasion of TSCC through the Hippo-TAZ signaling pathway.

Introduction

Tongue squamous cell carcinoma (TSCC) is one of the most common cancer types of the head and neck, often resulting in short survival times and poor prognosis (1). At present, treatment of TSCC involves a comprehensive therapeutic model combining surgery, radiation and chemotherapy (2-5). However, chemical agents kill not only tumor cells but also normal cells, thereby exhibiting cellular toxicity, along with the possibility of inducing resistance in tumor cells (6). Therefore, the identification of highly efficient, low toxicity targeting drugs from natural sources has gradually become a topic of contemporary research. In recent years, the primary extract from green tea epigallocatechin-3-gallate (EGCG) has demonstrated anti-tumor bioactivities with mild side effects in normal cells (7,8). In addition, attention has been focused on targeted therapy against molecules, including epidermal growth factor receptor (EGFR), cyclooxygenase-2 (COX-2), peroxisome proliferator-activated receptor-γ (PPARγ) and progesterone receptor, to treat oral cancer (9). Numerous *in vitro* studies have reported the abilities of EGCG to reduce growth, induce apoptosis, and inhibit the migration and invasion of TSCC cell lines through several molecular signaling pathways (10-16). The Hippo signaling pathway is a highly conserved signaling pathway. When this pathway is activated, its downstream transcription coactivator with a PDZ-binding motif tafazzin (TAZ) is translocated into the nucleus to bind the TEA domain transcription factor family, and induce changes in the expression of a range of genes associated with proliferation, survival and migration (17,18). According to previous studies, the activation of Hippo-TAZ signaling promotes proliferation, migration and invasion, and inhibits apoptosis in TSCC cells (19,20). However, the effect EGCG on TAZ expression has not been well evaluated in human TSCC cells. Thus, the present study aimed to explore the possible associations between EGCG stimulation and activation of the Hippo-TAZ signaling pathway in TSCC cells.

Therefore, the current study was performed to investigate how EGCG exerts its biological effects on processes, including cell proliferation, apoptosis, migration and invasion through the Hippo-TAZ signaling pathway in TSCC cells.

Materials and methods

Reagents and antibodies. EGCG (E8120) was purchased from Beijing Solarbio Science & Technology Co., Ltd. (Beijing,

Correspondence to: Dr Yong Wen, Department of Implantology, School of Stomatology, Shandong University, 44-1 Wenhua Xi Road, Jinan, Shandong 250012, P.R. China
E-mail: wenyong@sdu.edu.cn

China). Simvastatin (S6196) was purchased from Merck KGaA (Sigma-Aldrich; Darmstadt, Germany) and dissolved in DMSO to make stock solutions. Primary rabbit mono-clonal anti-human antibodies against TAZ (cat. no., 70148), phosphorylated (p)-TAZ (Ser89) (cat. no., 59971), large tumor suppressor 1 (LATS1; cat. no., 3477), MOB kinase activator 1 (MOB1; cat. no., 13730), mammalian sterile 20-like 1 (MST1; cat. no., 14946), salvador 1 (SAV1; cat. no., 13301), c-Jun N-terminal kinase (JNK; cat. no., 9252), p-JNK (Thr183/Tyr185) (cat. no., 4668), extracellular regulated protein kinases (Erk; cat. no., 4695), p-Erk (Thr202/Tyr204) (cat. no., 4370), protein kinase B (Akt) (cat. no., 4691), p-Akt (Ser473) (cat. no., 4060), B cell lymphoma-2 (Bcl-2; cat. no., 2872), Bcl-2 associated X protein (Bax; cat. no., 5023), poly ADP-ribose polymerase (PARP; cat. no., 9532), cleaved PARP (cat. no., 5625), vimentin (cat. no., 5741), and E-cadherin (cat. no., 3195), GAPDH (cat. no., 5174) were purchased from Cell Signaling Technology, Inc. (Danvers, MA, USA). Horseradish peroxidase (HRP)-conjugated goat anti-rabbit secondary antibodies were obtained from Affinity Biosciences (cat. no., S0001; Cincinnati, OH, USA).

Cell lines and culture. The TSCC cell lines, CAL27 and SCC15, were obtained from the American Type Culture Collection (Manassas, VA, USA). They were identified using short tandem repeats. CAL27 cells were cultured in Dulbecco's modified Eagle's medium (HyClone; GE Healthcare Life Sciences, Logan, UT, USA), while SCC15 cells were incubated in minimum essential medium (HyClone; GE Healthcare Life Sciences) supplemented with 10% fetal bovine serum (FBS; Gibco; Thermo Fisher Scientific, Inc., Waltham, MA, USA) and 1% penicillin-streptomycin at 37˚C in a humidified atmosphere with 5% CO_2.

Proliferation assay. Cell proliferation was measured by a Cell-Counting Kit-8 assay (Dojindo Molecular Technologies, Inc., Kumamoto, Japan). Cells were cultured in 96-well tissue culture plates (4.0×10^3 cells/well) with 10% FBS for 24 h. Then, the cells were exposed to different concentrations of EGCG (0, 40, 80, 120, 160 and 200 μM) for different durations (0, 24, 48, 72, 96 and 120 h). Following incubation, 10 μl CCK-8 solution was added to each well, and the plates were incubated for an additional 2 h. The absorbance was measured using a spectrometer at a wavelength of 450 nm.

Cell proliferation was also assessed using an EdU Apollo *in vitro* kit (Guangzhou RiboBio Co., Ltd., Guangzhou, China) following the manufacturer's protocol. CAL27 cells were seeded at a density of 1.0×10^5 cells/cm^2 in 24-well plates and incubated for 24 h in normal growth medium. Cells were treated with 200 μl EdU for 2 h and then fixed with 4% paraformaldehyde for 15-20 min at room temperature. The cells were then incubated with 2 mg/ml glycine at room temperature for 10 min, followed by washing with PBS. Then, the cells were permeabilized with 100 μl/well permeabiliza-tion buffer (0.5% Triton X-100 in PBS) at room temperature for 30 min and incubated with 200 μl 1X Apollo solution for 30 min at room temperature in the dark. Subsequently, the cells were incubated with 200 μl 1X Hoechst 33342 solution for 30 min at room temperature in the dark. The percentage of EdU-positive cells was determined by fluorescence microscopy

(magnification, x100) and was calculated using Image-Pro Plus 6.0 software (Media Cybernetics Inc., Rockville, MD, USA).

Apoptosis assay. Cell apoptosis was analyzed by flow cytometry. Cells with green fluorescent probes and empty vector were stained using the Annexin V-APC staining kit (Sungene Biotech Co., Ltd., Tianjin, China). Briefly, following washing with cold PBS, the cells were suspended in 500 μl 1X binding buffer, and then incubated with 5 μl Annexin V-fluorescein APC at room temperature in the dark for 10 min. Finally, 5 μl 7-AAD solution was added and cells were incubated for 5 min at room temperature in the dark. Untreated control cells without transfection were measured using the Annexin V-FITC/PI kit [Hangzhou Multi Sciences (Lianke) Biotech Co., Ltd., Hangzhou, China] following the manufacturer's protocol. The percentage of apoptotic cells was measured using a FACSCalibur (BD Biosciences, San Jose, CA, USA), and analyzed using CellQuest software version 5.1 (BD Biosciences).

Wound healing assay. Cells (8.0×10^5/well) were seeded in 6-well plates, and allowed to attach and reach 80% confluence. Cell monolayers were wounded by scratching with 200-μl pipette tips and then washed twice with PBS to remove floating cells. Cells in each well were subsequently exposed to FBS-free medium with or without EGCG for up to 48 h. Cells were imaged at x100 magnification with a phase-contrast micro-scope at each time point. The wound healing areas at different time points were measured using ImageJ software 14.8 for Windows (National Institutes of Health, Bethesda, MD, USA).

Transwell invasion assay. Cells (1.0×10^4 cells/well) were seeded in the upper chamber of Transwell inserts (8-μm pore size) pre-coated with Matrigel (both from Corning Incorporated, Corning, NY, USA) and exposed to FBS-free medium with or without different concentrations of EGCG. Medium containing 10% FBS was placed in the lower chamber, and cells for each treatment were incubated for 24 h at 37˚C in a humidified environment with 5% CO_2. Then, non-invaded cells in the upper chamber were removed with a cotton swab, and invaded cells were washed with PBS, fixed with 4% para-formaldehyde for 30 min and stained with 0.1% crystal violet (Solarbio, Shanghai, China) for 10 min. Images were captured with a light microscope at x200 magnification, and the number of cells that had penetrated the membrane was counted using Image-Pro Plus 6.0 software.

Cell transfection. A total of 1×10^6 CAL27 cells were seeded and transfected at ~80% confluence with culture medium with 8 μg/ml Polybrene and 100 μl overexpression TAZ lentivirus particle LV5-homo-TAZ (NM_000116.4) (TAZ-overexpression group). Similarly, CAL27 cells at ~80% confluence were transfected with the culture medium with 8 μg/ml Polybrene and 100 μl empty vector lentivirus LV5-NC (NM_000116.4) (negative control group). After 6-8 h, the medium was changed to basal medium (HyClone; GE Healthcare Life Sciences) supplemented with 10% FBS, and the cells were cultured for further analyses. The effi-ciency of TAZ overexpression was determined using western
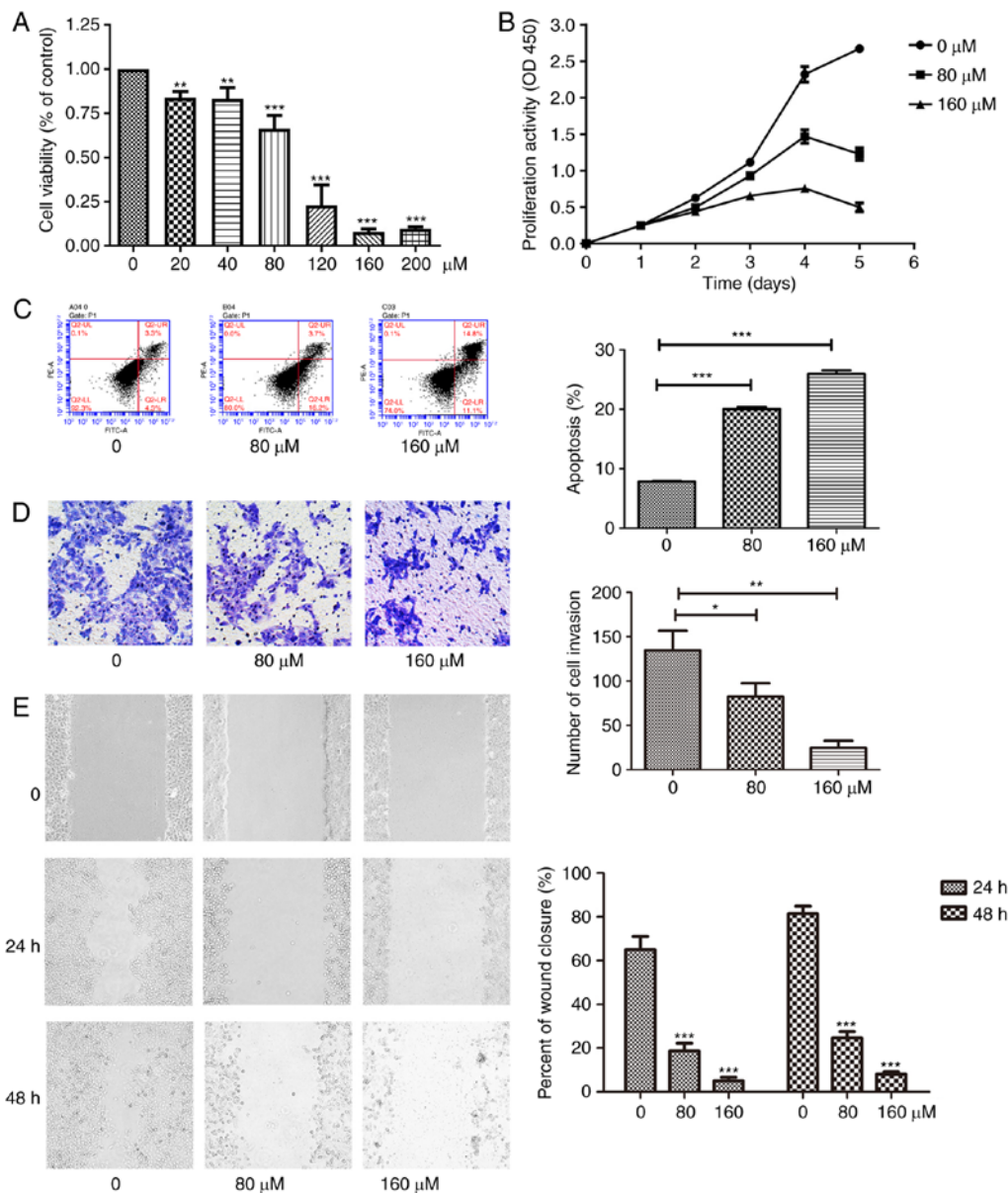
Figure 1. EGCG inhibits the proliferation, migration and invasion of CAL27 cells in a dose-dependent manner. (A) Cells were exposed to increasing concentrations of EGCG (0-200 μM) for 24 h. Following treatment, cell viability was measured using a CCK-8 assay. (B) Cell growth was measured by CCK-8 assay at the indicated time points and EGCG concentrations. (C) Cell apoptosis was determined by flow cytometry after 24 h of treatment, and the rates of apoptosis at different EGCG concentrations were statistically analyzed. (D) Cell invasion was measured using a Transwell assay in response to treatment with different concentrations of EGCG for 24 h (magnification, x200). (E) Cell migration was analyzed using scratch assay following treatment with the indicated concentration of EGCG treatment for 24 and 48 h (magnification, x100) and the percentage of wound closure was statistically analyzed. *P<0.05, **P<0.01 and ***P<0.001, vs. the control (0 μM) group or as indicated. EGCG, epigallocatechin-3-gallate; CCK-8, Cell Counting Kit-8.

blotting and reverse transcription-quantitative polymerase chain reaction (RT-qPCR) assays.

Total protein isolation and western blotting. Cells were collected and lysed in ice-cold RIPA lysis buffer (Beyotime Institute of Biotechnology, Shanghai, China), and the concentration of each protein sample was quantified using a bicinchoninic acid assay. Subsequently, 20 μg of protein from each sample was separated using 10% SDS-PAGE and transferred onto polyvinylidene difluoride membranes (EMD Millipore, Billerica, MA, USA). Following blocking in 5% fat-free milk for 1 h at room temperature, the membranes were probed with primary antibodies (dilution 1:1,000) at 4˚C overnight. Next, they were washed with Tris-based saline-Tween-20 (20 mmol/l Tris-HCl, 150 mmol/l NaCl and 0.05% Tween-20) at room temperature three times for 10 min each. Then, the membranes were incubated with HRP-conjugated secondary antibodies (dilution 1:20,000) at room temperature for 1 h. Finally, protein bands were detected using the Immobilon Western chemiluminescent HRP substrate kit (EMD Millipore). Quantitative analysis of protein bands was calculated using ImageJ with 64-bit Java 1.6.0-24 program for Windows.

RNA isolation and RT-qPCR. Total RNA was extracted from cells at 80% confluence using TRIzol® reagent (Gibco; Thermo Fisher Scientific, Inc.) and then reverse transcribed into
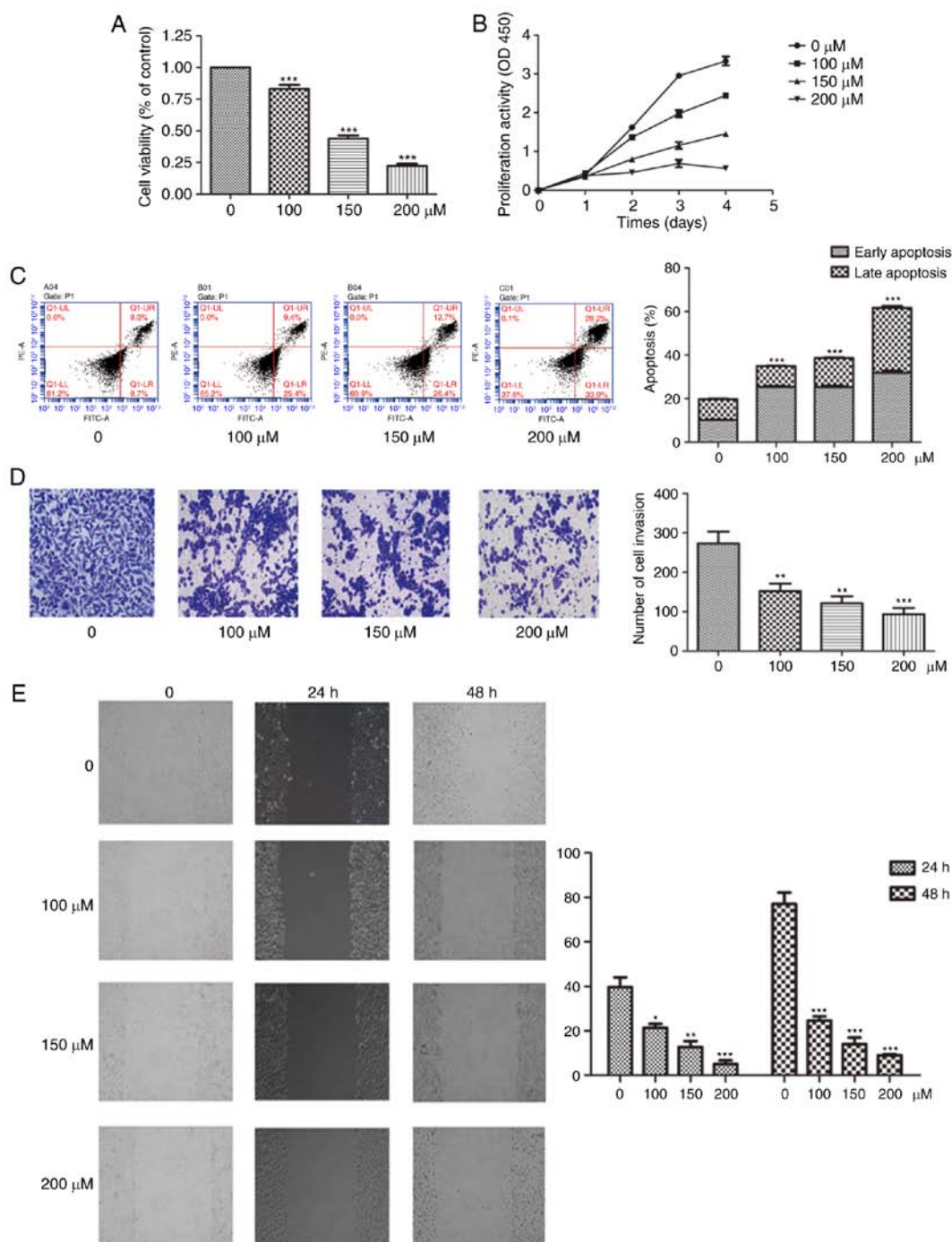
Figure 2. EGCG inhibits the proliferation, migration and invasion of SCC15 cells in a dose-dependent manner. (A) Cells were exposed to increasing concentrations of EGCG (0-200 μM) for 24 h. Following treatment, cell viability was measured using a CCK-8 assay. (B) Cell growth was measured by CCK-8 assay at the indicated time points and EGCG concentrations. (C) Cell apoptosis was determined by flow cytometry after 24 h of treatment, and the rates of apoptosis at different EGCG concentrations were statistically analyzed. (D) Cell invasion was measured using a Transwell assay in response to treatment with different concentrations of EGCG for 24 h (magnification, x200). (E) Cell migration was analyzed using scratch assay following treatment with the indicated concentration of EGCG treatment for 24 and 48 h (magnification, x100), and the percentage of wound closure was statistically analyzed. *P<0.05, **P<0.01 and ***P<0.001, vs. the control (0 μM) group or as indicated. EGCG, epigallocatechin-3-gallate; CCK-8, Cell Counting Kit-8.

cDNA using the PrimeScript™ RT II reagent kit (Takara Bio, Inc., Otsu, Japan) according to manufacturer's protocol. The generated cDNA was used as template for Quantitative real-time PCR (RT-qPCR) using SYBR Premix Ex Taq™ kit (Takara, Tokyo, Japan) following the manufacturer's protocol. Amplification conditions were as follows: Initial step of 95°C for 30 sec; 45 cycles of 95°C for 5 sec, 60°C for 35 sec and 72°C for 60 sec; and a final step at 40°C for 30 sec. RT-qPCR was performed using a LightCycler® 480 II and changes in gene expression were calculated using the $2^{-\Delta\Delta Cq}$ method (21). The expression levels of GAPDH and TAZ were analyzed and the primers used in the present study were as follows: TAZ forward, 5'-GCTGCTTCTGGACCAAGTACA-3' and reverse, 5'-AGATGTGGCGGAGTTTCAGG-3'; GAPDH forward, 5'-GCTTGTCATCAACGGGAAG-3' and reverse, 5'-GAT GTTAGTGGGGTCTCG-3'.
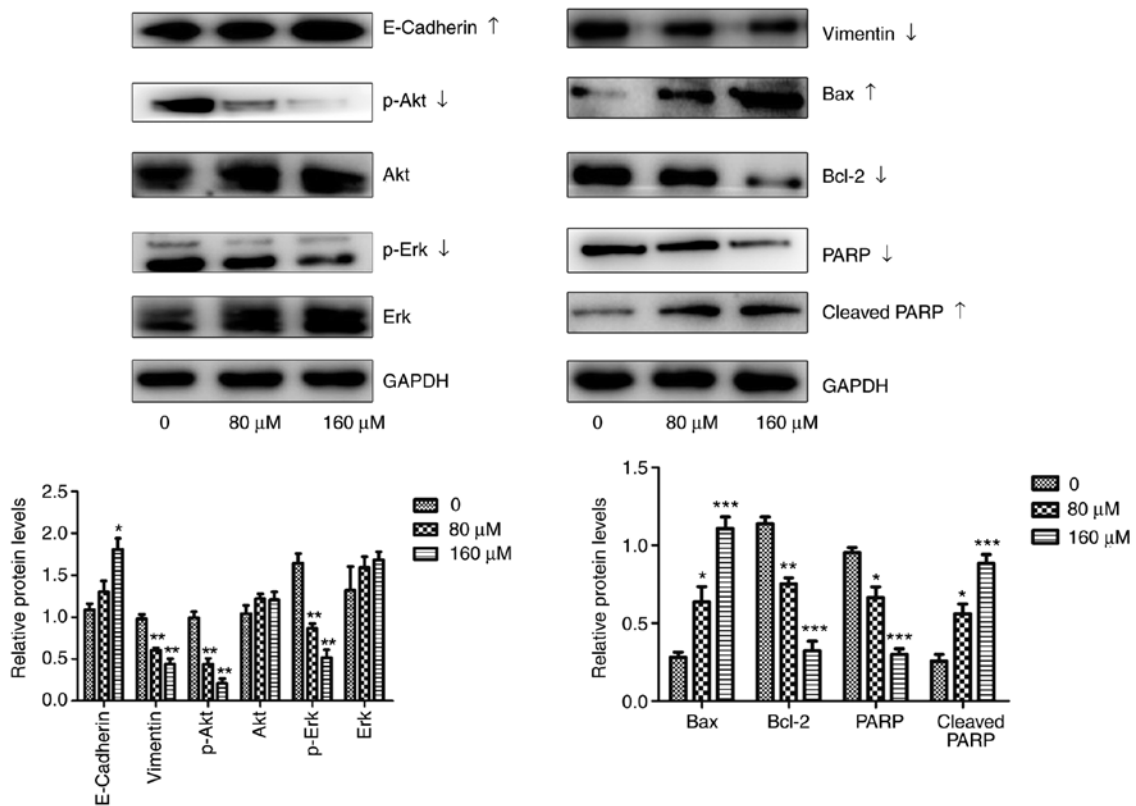
Figure 3. EGCG affects the expression of genes associated with proliferation, apoptosis and EMT in CAL27 cells. Changes in Erk, p-Erk, Akt, p-Akt, Bcl-2, Bax, PARP, cleaved PARP, vimentin, E-cadherin and GAPDH expression were determined using a western blot assay after 24 h of treatment with different concentrations of EGCG. All data are presented as the mean ± standard deviation from three experiments. *P<0.05, **P<0.01 and ***P<0.001, vs. the control (0 μM) group. EMT, epithelial-mesenchymal transition; Erk, extracellular regulated protein kinases; p-Erk, phosphorylated Erk; Akt, protein kinase B; p-Akt, phosphorylated Akt; Bcl-2, B cell lymphoma/lewkmia-2; Bax, Bcl-2 associated X protein; PARP, poly ADP-ribose polymerase; EGCG, epigallocatechin-3-gallate.

Statistical analysis. All statistical analyses were performed using GraphPad Prism 5.0 software (GraphPad Software, Inc., La Jolla, CA, USA). Differences between multiple groups were examined using one-way analysis of variance followed by Tukey's post hoc test and a two-tailed t-test was used for the comparison between two groups. All results are expressed as the mean ± standard deviation from at least three independent experiments. P<0.05 was considered to indicate a statistically significant difference.

Results

EGCG stimulation inhibits proliferation, migration and invasion, and promotes apoptosis in CAL27 and SCC15 cells. To investigate the effect of EGCG on proliferation of CAL27 cells, cells were treated with different concentrations of EGCG and the changes in proliferation were measured using a CCK-8 assay. Cell proliferation was significantly decreased in response to EGCG treatment in time- and dose-dependent manners (Fig. 1A and B). Following incubation for 120 h, the cell numbers in the 160 μM EGCG group were significantly lower compared with those in the control groups. Eventually, 80 μM was established as the optional drug concentration. Additionally, cell apoptosis was measured by flow cytometry (Fig. 1C). The apoptosis rates, total and early apoptosis, of the 80 μM EGCG group were significantly higher compared

with those of the group without EGCG. In addition, the 160 μM EGCG group had a higher proportion of cells in late apoptosis compared with the 80 μM EGCG group. EGCG also significantly inhibited cell invasion in a concentration-dependent manner as evaluated using a Transwell assay (Fig. 1D). Similarly, as revealed using the scratch assay, EGCG significantly reduced the time of wound healing (Fig. 1E). Therefore, the results of the present study indicated that EGCG inhibited proliferation, migration and invasion, and promoted apoptosis in CAL27 cells. In order to confirm these findings, the aforementioned experiments were repeated in SCC15 cells, whereby similar changes were observed (Fig. 2)

EGCG causes changes in the expression of genes associated with proliferation, apoptosis and epithelial mesenchymal transition (EMT) in CAL27 cells. Western blot assays were performed to confirm whether EGCG treatment induces changes in the expression of proteins associated with proliferation, apoptosis, migration and invasion (Fig. 3). Akt is known as a key molecule of the PI3K/Akt/MTOR signaling pathway (22), and Erk-1/2 is a component of the mitogen-activated protein kinase (MAPK) signaling pathway (23), which affects the expression of proliferation-associated proteins. According to the results of the present study, EGCG significantly reduced the expression of proliferation-associated proteins compared with normal (0 μM) cells, including p-Akt, while no differences
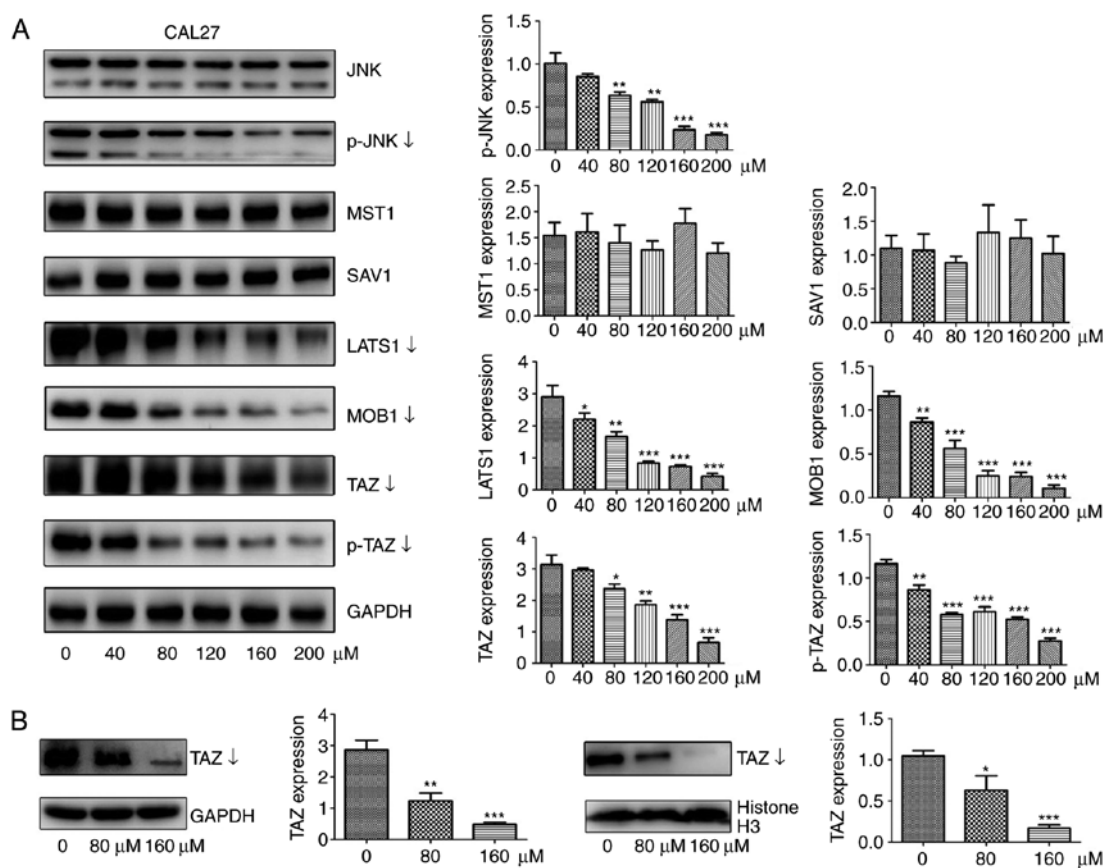
Figure 4. EGCG downregulates the protein expression of TAZ, LATS1, MOB1 and JNK in CAL27 cells. (A) Western blot analysis was used to measure the protein abundance of JNK, p-JNK, p-TAZ, TAZ, LATS1, MOB1, SAV1, and MST1 in response to treatment with different concentrations of EGCG for 24 h. (B) Protein levels of TAZ in nuclear or cytoplasmic lysates determined by western blotting following treatment with different doses of EGCG for 24 h. Histone H3 and GAPDH served as internal controls for nuclear and cytoplasmic proteins, respectively. All data are presented as the mean ± standard deviation from three experiments. $^{*}P<0.05$, $^{**}P<0.01$ and $^{***}P<0.001$, vs. the control (0 μM) group. TAZ, tafazzin; p-TAZ, phosphorylated TAZ; LATS1, large tumor suppressor 1; MOB1, MOB kinase activator 1; SAV1, salvador 1; MST1, mammalian sterile 20-like 1; JNK, c-Jun N-terminal kinase; p-JNK, phosphorylated JNK; EGCG, epigallocatechin-3-gallate.

were observed in total Akt expression. Although the level of total Erk was unaffected, changes in p-Erk levels indicate a reduction in proliferative abilities.

The apoptotic pathway is tightly regulated by pro- and anti-apoptotic members of the Bcl-2 protein family (24). Bcl-2 is an anti-apoptotic protein of the Bcl-2 family, whereas Bcl-2 associated X apoptosis regulator is a pro-apoptotic protein of the same family. PARP is a zinc-finger DNA-binding enzyme that is activated by binding to DNA breaks. When it is activated, PARP is cleaved (25). It has been reported that EMT affects tumor metastasis (26), and the expression of proteins associated with EMT in the present study changed in response to EGCG treatment, indicating that EGCG serve a role in tumor metastasis. The expression of E-cadherin, an epithelial protein, significantly increased with EGCG treatment compared with untreated control cells. In contrast, the expression of vimentin, a mesenchymal protein, significantly decreased in response to EGCG treatment.

EGCG downregulates Hippo-TAZ signaling, and the expression of associated upstream genes in CAL27 and SCC15 cells. In previous studies, researchers have demonstrated that TAZ is associated with tumorigenesis-associated processes in TSCC, including cell proliferation, survival and

migration *in vitro* (19,20). Therefore, whether the expression of TAZ and its upstream signaling molecules were affected by EGCG treatment were investigated in the present study. As expected, the protein levels of total TAZ and p-TAZ were significantly decreased in response to different doses of EGCG for 24 h of CAL27 cells (Fig. 4A). To investigate whether EGCG altered the nuclear localization of TAZ, proteins were extracted from the nucleus and cytoplasm of cells, and the relevant protein levels of TAZ were decreased in parallel with total TAZ levels (Fig. 4B). Next, the effect of EGCG on the upstream signaling pathway was determined. As determined by the western blot assay, EGCG treatment significantly decreased LATS1 and MOB1 protein levels compared with untreated control cells. However, EGCG had minimal or no effect on MST1 and SAV1 expression (Fig. 4A). Next, total JNK and p-JNK protein levels were examined. p-JNK levels were significantly decreased while total JNK level remained constant (Fig. 4A) compared with untreated control cells, consistent with the results of a previous study (10). In order to confirm these findings, all the aforementioned experiments were performed on SCC15 cells, whereby Hippo-associated proteins and p-JNK protein exhibited the same trend as CAL27 cells, indicating that EGCG inhibited the biological behaviors of TSCC through the Hippo-TAZ signaling pathway (Fig. 5).
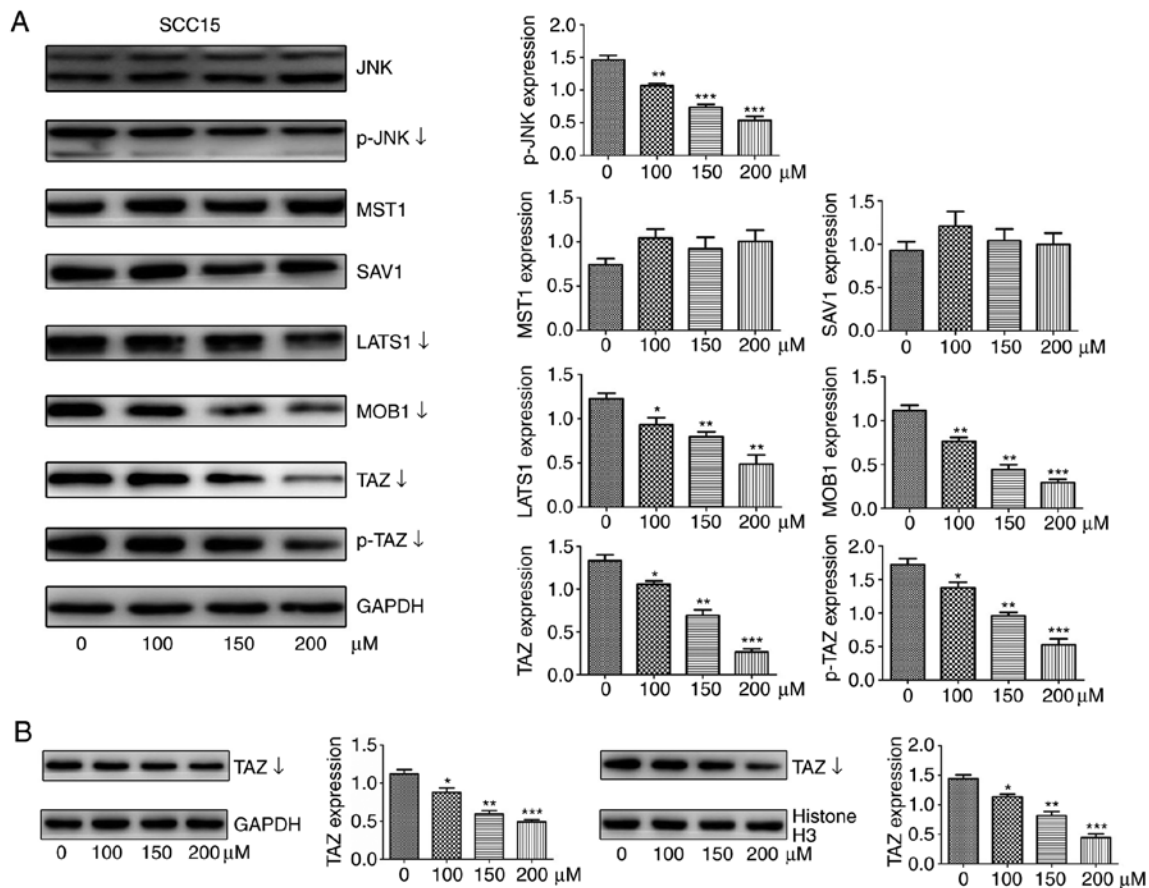
Figure 5. EGCG downregulates the protein expression of TAZ, LATS1, MOB1 and JNK in SCC15 cells. (A) Western blot analysis was used to measure the protein abundance of JNK, p-JNK, p-TAZ, TAZ, LATS1, MOB1, SAV1, and MST1 in response to treatment with different concentrations of EGCG for 24 h. (B) Protein levels of TAZ in nuclear or cytoplasmic lysates determined by western blotting following treatment with different doses of EGCG for 24 h. Histone H3 and GAPDH served as internal controls for nuclear and cytoplasmic proteins, respectively. All data are presented as the mean ± standard deviation from three experiments. *P<0.05, **P<0.01 and ***P<0.001, vs. the control (0 μM) group. TAZ, tafazzin; p-TAZ, phosphorylated TAZ; LATS1, large tumor suppressor 1; MOB1, MOB kinase activator 1; SAV1, salvador 1; MST1, mammalian sterile 20-like 1; JNK, c-Jun N-terminal kinase; p-JNK, phosphorylated JNK; EGCG, epigallocatechin-3-gallate.

TAZ overexpression attenuates the effects of EGCG on CAL27 cells. To investigate whether the expression level of TAZ influenced EGCG-treated cells, CAL27 cells were treated with TAZ overexpression lentiviral particles or control lentiviral particles for another 24-48 h. Western blot analysis and RT-qPCR assays indicated the successful overexpression of TAZ (Fig. 6A and B). Treatment with EGCG significantly inhibited proliferation, migration and invasion and promoted apoptosis in control cells. However, TAZ overexpression alleviated the effects of EGCG compared with that in EGCG-treated control cells (Fig. 6C-G). No significant differences were observed in the protein expression levels between the empty vector group and non-transfected cell group, which were all stimulated with EGCG, indicating that the transfection of control lentiviral particles exhibited little influence on CAL27 cells. The protein levels of TAZ, Bcl-2, p-Akt and vimentin significantly increased in TAZ-overexpression cells, and E-cadherin protein significantly decreased compared with the non-transfected cells and the empty vector groups, which was in parallel with the morphological features observed (Fig. 7). Taken together, these results revealed that TAZ overexpression, at least in part, abolished the effects of EGCG, further demonstrating that the Hippo-TAZ pathway serves an important role in regulating CAL27 cell proliferation and migration in response to EGCG stimulation.

EGCG and simvastatin additively inhibit proliferation, migration and invasion, and promote apoptosis in CAL27 cells. Simvastatin, which has been identified as the inhibitor of TAZ, was used to treat CAL27 cells stimulated with EGCG (20). To further determine the additive effects of EGCG and simvastatin, CCK-8 assays, flow cytometry, scratch and Transwell assays were used to examine the corresponding changes in the proliferative, apoptotic, migrative and invasive abilities of CAL27 cells (Fig. 8). Simvastatin decreased the TAZ protein level in a dose manner, particularly at 20 μM, thus 20 μM was selected as the optional drug concentration (Fig. 8A). It was demonstrated that 80 μM EGCG and 20 μM simvastatin treatment separately inhibited the proliferation, migration and invasion of CAL27 cells, but more significant suppressive changes were detected when cells were treated with a combination of EGCG and simvastatin (Fig. 8B, C and E). In addition, 80 μM EGCG and 20 μM simvastatin promoted cell apoptosis to varying degrees, the simulative effect was more significant when cells were exposed to both drugs compared with single treatment (Fig. 8D).
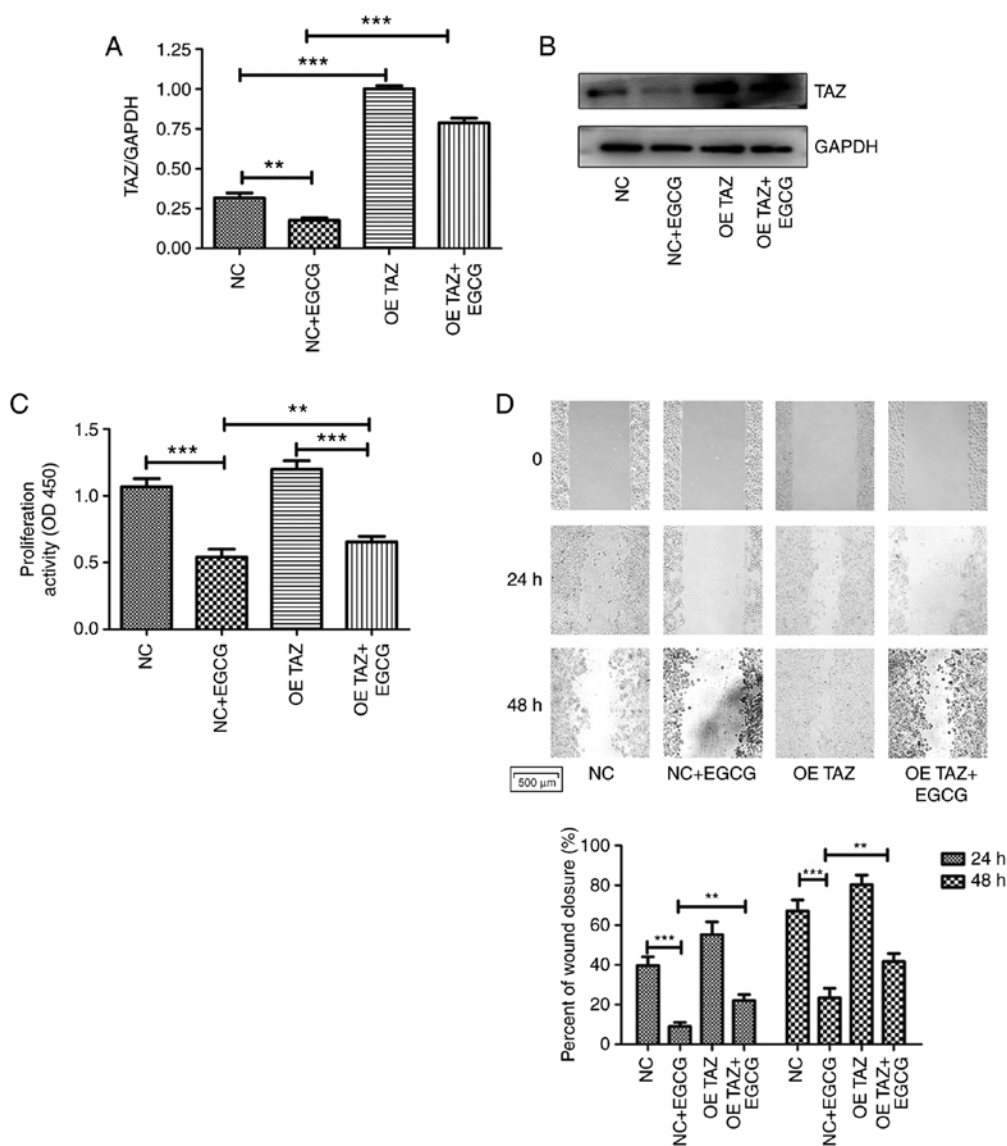
Figure 6. TAZ overexpression attenuates the effects of EGCG on CAL27 cells on processes, including proliferation, apoptosis, migration and invasion. (A) RT-qPCR and (B) western blot analysis demonstrated successful TAZ overexpression. (C) Proliferation was determined using Cell Counting Kit-8 assay. (D) Scratch assay was performed to determine cell migratory ability (top panel) and images of the migrating cells were analyzed (bottom image) (magnification, x100).

Discussion

Green tea is one of the most frequently and heavily consumed beverages worldwide (8). EGCG, as the primary active compound in green tea, accounting for 50-80% or 200-300 mg/brewed cup of green tea, has been extensively studied for its health benefits and anti-tumor properties (7,27,28). Notably, EGCG serves an important role in the prevention and treatment of oral cancer, likely via the mitochondrial pathway, and exerts little toxic effects on normal cells (29,30).

TSCC is one of the most common and malignant types of oral cancer, and it is significantly more malignant compared with other types of oral squamous cell carcinoma (OSCC) because the tongue is an active organ with an abundant blood supply (31). Therefore, patient with TSCC typically have a poor prognosis following systematic therapy (32). At present, targeted therapy may be a novel therapeutic approach to prevent the occurrence and development of TSCC (9). Previous studies have demonstrated that EGCG exerts an anti-tumor effect by suppressing the turnover and enhancing the degradation of β-catenin (14,15). In addition, other studies have demonstrated that EGCG treatment induces apoptosis in human OSCC cells by suppressing hepatocyte growth factor c-Met signaling and downstream MAPK signaling pathways, and inhibits the proliferation of OSCC cells by upregulating Bcl-2 via p38 and Erk signaling (10,11,13,33).

TAZ, a key effector of the Hippo signaling pathway, is a novel oncogene with pleiotropic roles in TSCC tumorigenesis (34,35). Notably, TAZ promotes cell proliferation, migration and invasion, as well as EMT, and prevents apoptosis in oral cancer (19,20,36). However, there is little research on the association between EGCG and TAZ in TSCC cells.

In the present study, the human TSCC cell lines CAL27 and SCC15 were used as research models, and whether EGCG stimulation was able to inhibit the proliferation, migration and invasion, and increase apoptosis was determined in accordance with the results of previous studies (11,37-39). The changes in the expression of markers of proliferation, apoptosis, invasion
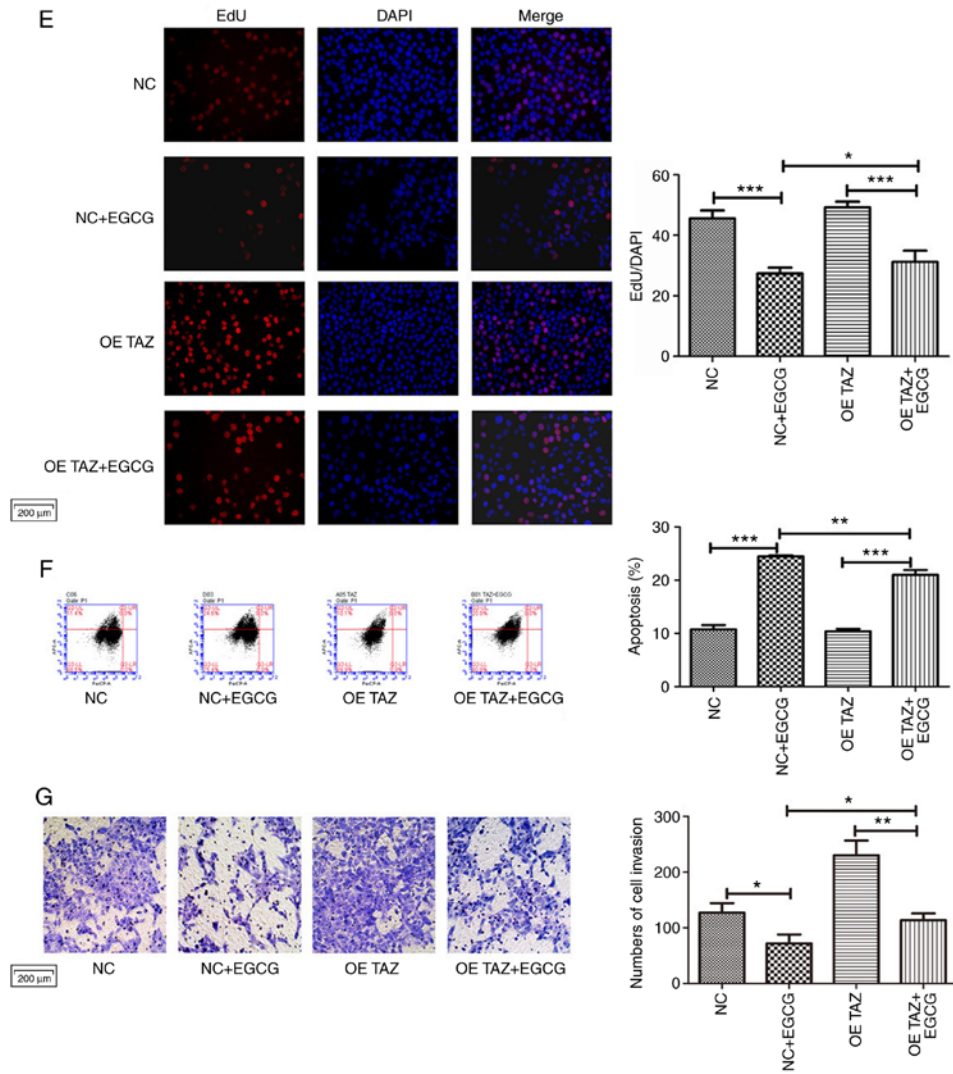
Figure 6. Continued. (E) Cell proliferation was also determined using an EdU assay. Images of proliferating CAL27 cells following various treatments were statistically analyzed (magnification, x200). (F) Apoptosis was analyzed by flow cytometry. (G) Invasion was evaluated using a Transwell assay (magnification, x200). *P<0.05, **P<0.01 and ***P<0.001. NC, negative control group; OE TAZ, TAZ overexpression group; TAZ, tafazzin; EGCG, epigallocatechin-3-gallate.
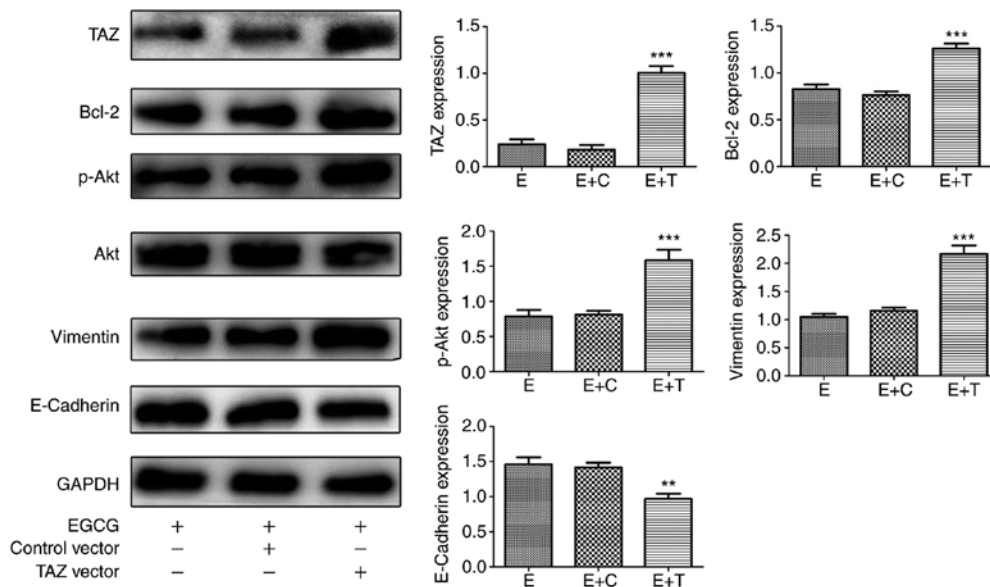

Figure 7. TAZ-overexpressing cells are more resistant to EGCG challenge compared with negative control or normal cells in CAL27 cells. Protein levels of TAZ, Bcl-2, Akt, p-Akt, E-cadherin, Vimentin, and GAPDH were determined using western blot assay. All data are presented as the mean ± standard deviation from three experiments. **P<0.01 and ***P<0.001, vs. the EGCG group. E, EGCG; E+T, EGCG+TAZ vector; E+C, EGCG+control vector; TAZ, tafazzin; Bcl-2, B cell lymphoma/lewkmia-2; Akt, protein kinase B; p-Akt, phosphorylated Akt; EGCG, epigallocatechin-3-gallate.
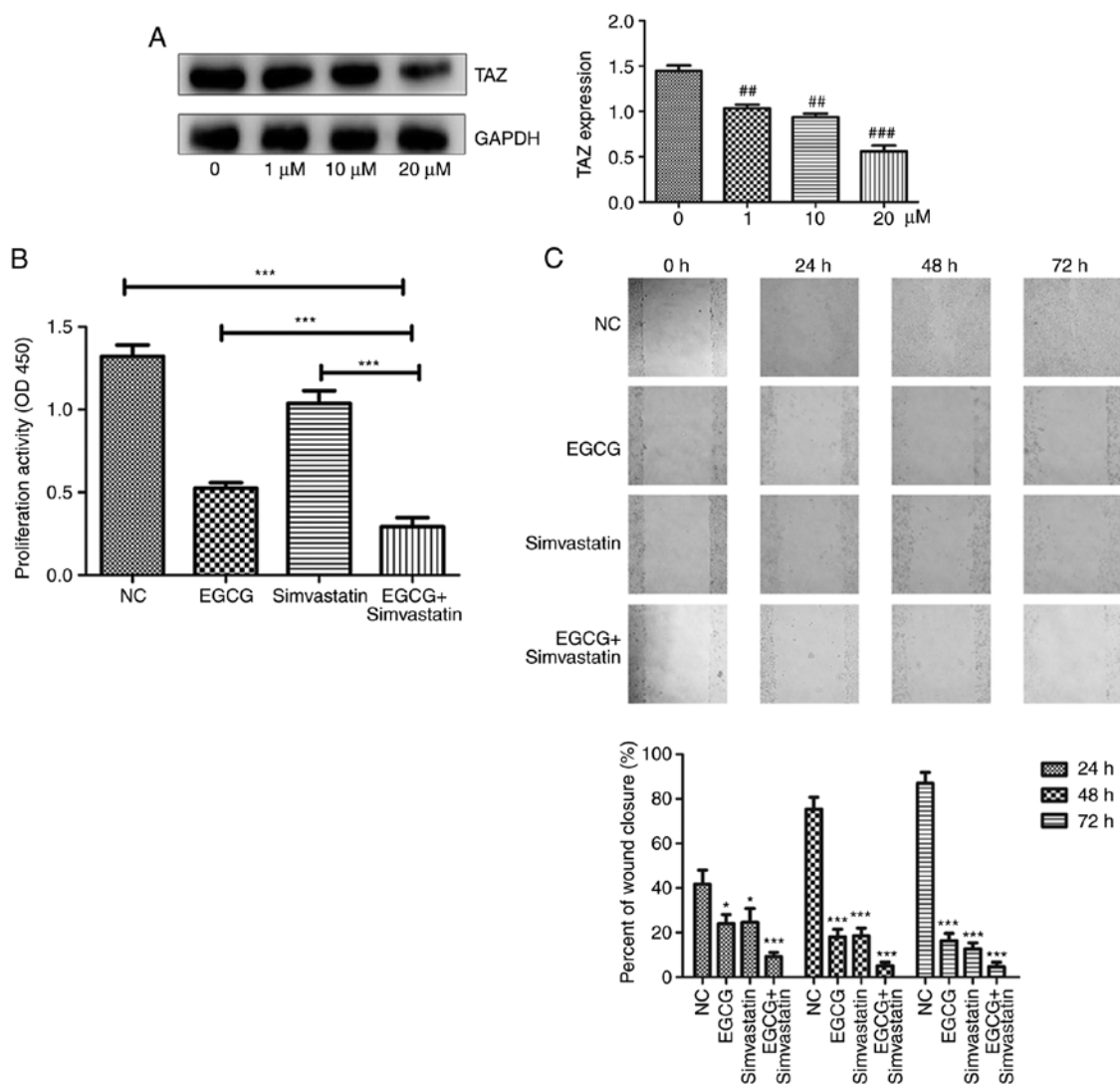
Figure 8. EGCG and simvastatin additively inhibit proliferation, migration and invasion, and increase apoptosis in CAL27 cells under different conditions. (A) Simvastatin inhibited the protein expression of TAZ in a dose-dependent manner. ##$P<0.01$ and ###$P<0.001$, vs. the control (0 μM) group. (B) Cell proliferation was determined using a Cell Counting Kit-8 assay. (C) Scratch assay was used to detect cell migration (top panel), and the percent of wound closure was statistically analyzed (bottom image) (magnification, x100). *$P<0.05$, ***$P<0.001$, vs. NC group.

and migration further confirmed the phenotypic changes upon EGCG exposure.

Mechanistically, EGCG significantly decreased the protein levels of TAZ in a concentration-dependent manner in the cytoplasm and nucleus of CAL27 as well as SCC15 cells. Additionally, the protein level of p-TAZ decreased with increasing concentrations of EGCG. The protein levels of MOB1, LATS1, SAV1 and MST1 were also evaluated, which are relevant upstream genes of Hippo signaling, and similar changes were observed as TAZ in MOB1 and LATS1 levels. However, EGCG had minimal or no effect on MST1 and SAV1 expression. Following hippo signal activation, MST1/2 and SAV1 are phosphorylated, and subsequently phosphorylate LATS1/2 and MOB1 (40). Similar to MST1/2 and SAV1, two groups of mitogen-activated protein kinase kinase kinase (MAP4Ks), MAP4K1/2/3/5 and MAP4K4/6/7, also directly phosphorylate LATS1/2 at their hydrophobic motifs, and promote LATS1/2 activation (40,41). MAPK cascades classically involve mitogen-activated protein kinase kinase

kinase, mitogen-activated protein kinase kinase, MAPK and occasionally an upstream MAP4K (42). The MAPK signaling pathway is known to be tightly associated with cell proliferation and differentiation, among others, and this signaling cascade consists of p38, JNK, ERK and ERK5. Among these effectors, researchers reported that there may be associations between Hippo signaling and JNK through the Ajuba family (43). When JNK is activated, it promotes the phosphorylation of Ajuba proteins, which then bind strongly to LATS and occupy the phosphorylation site of LATS (43). Therefore, the protein levels of JNK and p-JNK were examined, and p-JNK was demonstrated to be decreased in a concentration-dependent manner, while JNK level remained invariable. These data suggest that EGCG serves an effective role through the phosphorylation of JNK, which then activates LATS and TAZ, but not through MST1/2 or SAV1.

Next, CAL27 cells were transfected with lentiviruses LV5-homo-TAZ and LV5-NC, and the cells were divided into a TAZ overexpression (OE TAZ) and a negative control (NC)
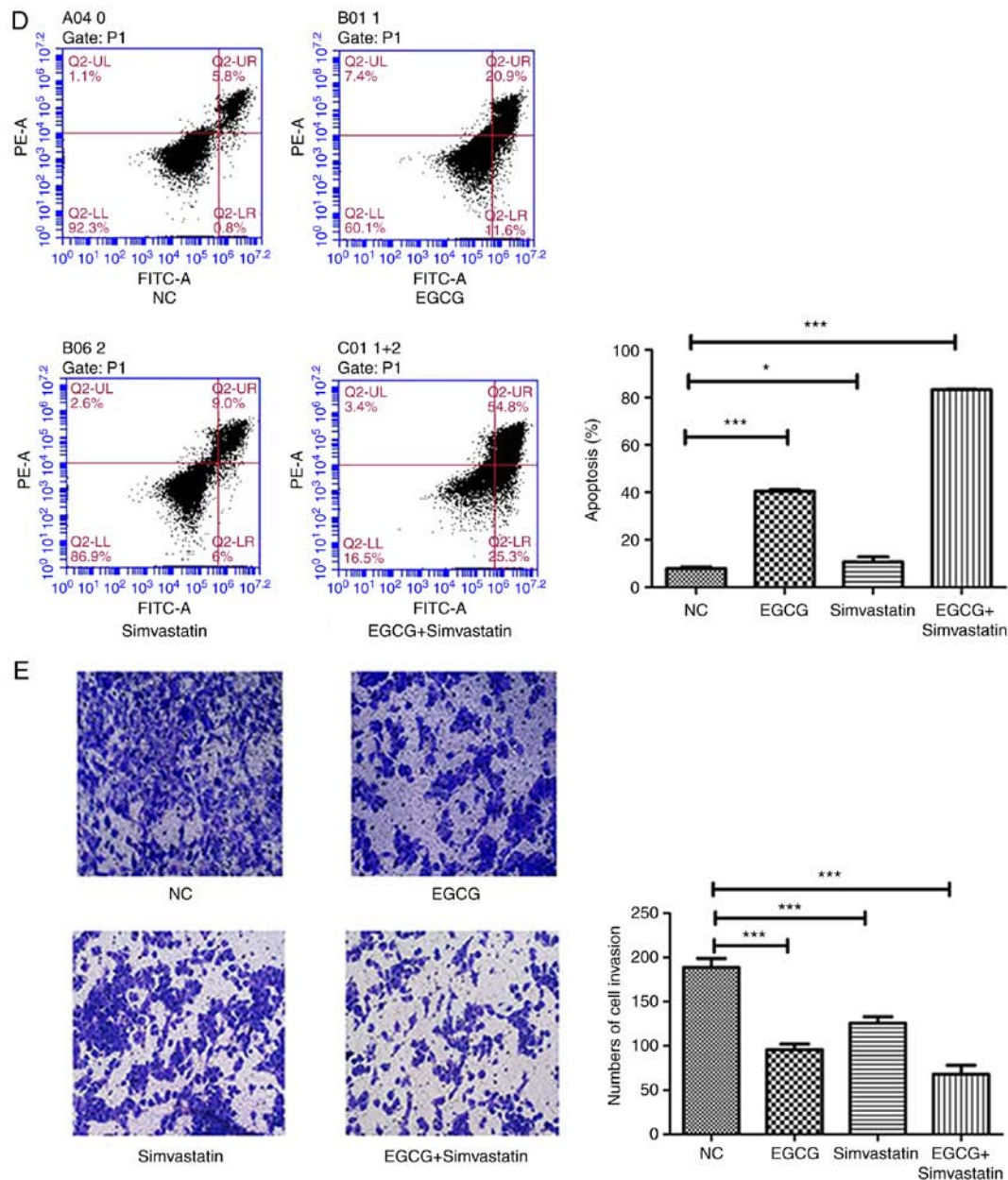
Figure 8. Continued. (D) Cells were incubated under different conditions for 24 h and then analyzed by flow cytometry to investigate apoptosis. (E) Transwell assay was performed to analyze cell invasion (magnification, x200). NC, negative control group; TAZ, tafazzin; EGCG, epigallocatechin-3-gallate. *P<0.05, ***P<0.001, vs. NC group.

groups. Indeed, EGCG inhibited the proliferation, migration and invasion, and increased apoptosis of the control group. However, TAZ overexpression alleviated the effects of EGCG on CAL27 cells compared with the EGCG-treated control group. Then, the changes in the expression of associated proteins were examined. As expected, the protein levels of TAZ, Bcl-2, p-Akt, E-cadherin and vimentin also paralleled the changes in morphological features.

To further verify that EGCG affects the biological characteristics of TSCC cells through the Hippo-TAZ pathway, a drug that has been shown to have similar bioactivities in CAL27 cells in a previous study was used (44). Simvastatin is a chemical inhibitor of the enzyme HMG-CoA reductase that catalyzes mevalonic acid production, and this effect may be attributed to other targets beyond Hippo-TAZ (45). A previous study

has reported that simvastatin reduces TAZ protein level in a concentration-dependent manner and that TAZ-overexpressing cells are more resistant to this compound compared with control cells (20). Thus, simvastatin was combined with EGCG. The combined treatment enhanced the corresponding phenotypic changes produced by single agent treatment. These data further demonstrate that EGCG affects the proliferation, apoptosis, migration and invasion of TSCC cells through the Hippo-TAZ signaling pathway.

In the present study, EGCG was demonstrated to the affect proliferation, apoptosis, migration and invasion of TSCC cells through the Hippo-TAZ signaling pathway. These results provide a molecular basis for the use of green tea as a potential chemotherapeutic agent in TSCC and offer more opportunities for molecular targeted therapy of TSCC.

Availability of data and materials

The datasets used during the present study are available from the corresponding author upon reasonable request.

Authors' contributions

KG and XC designed the experiments. AL performed the experiments. AL, KG, XC, QW, XF and YW analyzed the data, and AL wrote the manuscript. All authors were responsible for giving final approval of the version to be published.

Ethics approval and consent to participate

Not applicable.

Patient consent for publication

Not applicable.

Competing interests

The authors have declared that they have no competing interests.

Reference

1. Siegel RL, Miller KD and Jemal A: Cancer statistics, 2017. CA Cancer J Clin 67: 7-30, 2017.
2. Miller KD, Siegel RL, Lin CC, Mariotto AB, Kramer JL, Rowland JH, Stein KD, Alteri R and Jemal A: Cancer treatment and survivorship statistics, 2016. CA Cancer J Clin 66: 271-289, 2016.
3. Guidi A, Codecà C and Ferrari D: Chemotherapy and immunotherapy for recurrent and metastatic head and neck cancer: A systematic review. Med Oncol 35: 37, 2018.
4. Haddad RI and Shin DM: Recent advances in head and neck cancer. N Engl J Med 359: 1143-1154, 2008.
5. Ferris RL, Blumenschein G Jr, Fayette J, Guigay J, Colevas AD, Licitra L, Harrington K, Kasper S, Vokes EE, Even C, et al: Nivolumab for recurrent squamous-cell carcinoma of the head and neck. N Engl J Med 375: 1856-1867, 2016.
6. Colevas AD: Chemotherapy options for patients with metastatic or recurrent squamous cell carcinoma of the head and neck. J Clin Oncol 24: 2644-2652, 2006.
7. Afzal M, Safer AM and Menon M: Green tea polyphenols and their potential role in health and disease. Inflammopharmacology 23: 151-161, 2015.
8. Chen ZM and Lin Z: Tea and human health: Biomedical functions of tea active components and current issues. J Zhejiang Univ Sci B 16: 87-102, 2015.
9. Hamakawa H, Nakashiro K, Sumida T, Shintani S, Myers JN, Takes RP, Rinaldo A and Ferlito A: Basic evidence of molecular targeted therapy for oral cancer and salivary gland cancer. Head Neck 30: 800-809, 2008.
10. Chang CM, Chang PY, Tu MG, Lu CC, Kuo SC, Amagaya S, Lee CY, Jao HY, Chen MY and Yang JS: Epigallocatechin gallate sensitizes CAL-27 human oral squamous cell carcinoma cells to the anti-metastatic effects of gefitinib (Iressa) via synergistic suppression of epidermal growth factor receptor and matrix metalloproteinase-2. Oncol Rep 28: 1799-1807, 2012.
11. Irimie AI, Braicu C, Zanoaga O, Pileczki V, Gherman C, Berindan-Neagoe I and Campian RS: Epigallocatechin-3-gallate suppresses cell proliferation and promotes apoptosis and autophagy in oral cancer SSC-4 cells. Onco Targets Ther 8: 461-470, 2015.
12. Kanlaya R, Khamchun S, Kapincharanon C and Thongboonkerd V: Protective effect of epigallocatechin-3-gallate (EGCG) via Nrf2 pathway against oxalate-induced epithelial mesenchymal transition (EMT) of renal tubular cells. Sci Rep 6: 30233, 2016.
13. Lee JC, Chung LC, Chen YJ, Feng TH, Chen WT and Juang HH: Upregulation of B-cell translocation gene 2 by epigallocatechin-3-gallate via p38 and ERK signaling blocks cell proliferation in human oral squamous cell carcinoma cells. Cancer Lett 360: 310-318, 2015.
14. Oh S, Gwak J, Park S and Yang CS: Green tea polyphenol EGCG suppresses Wnt/β-catenin signaling by promoting GSK-3β- and PP2A-independent β-catenin phosphorylation/degradation. Biofactors 40: 586-595, 2014.
15. Shin YS, Kang SU, Park JK, Kim YE, Kim YS, Baek SJ, Lee SH and Kim CH: Anti-cancer effect of (-)-epigallocatechin-3-gallate (EGCG) in head and neck cancer through repression of transactivation and enhanced degradation of β-catenin. Phytomedicine 23: 1344-1355, 2016.
16. Masuda M, Wakasaki T, Toh S, Shimizu M and Adachi S: Chemoprevention of head and neck cancer by green tea extract: EGCG-The role of EGFR signaling and 'lipid raft'. J Oncol 2011: 540148, 2011.
17. Harvey KF, Zhang X and Thomas DM: The Hippo pathway and human cancer. Nat Rev Cancer 13: 246-257, 2013.
18. Pan D: The hippo signaling pathway in development and cancer. Dev Cell 19: 491-505, 2010.
19. Hiemer SE, Zhang L, Kartha VK, Packer TS, Almershed M, Noonan V, Kukuruzinska M, Bais MV, Monti S and Varelas X: A YAP/TAZ-regulated molecular signature is associated with oral squamous cell carcinoma. Mol Cancer Res 13: 957-968, 2015.
20. Li Z, Wang Y, Zhu Y, Yuan C, Wang D, Zhang W, Qi B, Qiu J, Song X, pagesYe J, et al: The Hippo transducer TAZ promotes epithelial to mesenchymal transition and cancer stem cell maintenance in oral cancer. Mol Oncol 9: 1091-1105, 2015.
21. Livak KJ and Schmittgen TD: Analysis of relative gene expression data using real-time quantitative PcR and the $2^{-\Delta\Delta C_T}$ method. Methods 25: 402-408, 2001.
22. Lim HJ, Crowe P and Yang JL: Current clinical regulation of PI3K/PTEN/Akt/mTOR signalling in treatment of human cancer. J Cancer Res Clin Oncol 141: 671-689, 2015.
23. Sun Y, Liu WZ, Liu T, Feng X, Yang N and Zhou HF: Signaling pathway of MAPK/ERK in cell proliferation, differentiation, migration, senescence and apoptosis. J Recept Signal Transduct Res 35: 600-604, 2015.
24. Siddiqui WA, Ahad A and Ahsan H: The mystery of BCL2 family: Bcl-2 proteins and apoptosis: An update. Arch Toxicol 89: 289-317, 2015.
25. Curtin NJ: PARP inhibitors for cancer therapy. In: Poly(ADP-Ribosyl)ation. Molecular Biology Intelligence Unit. Springer, Boston, MA, pp218-233, 2006.
26. Heerboth S, Housman G, Leary M, Longacre M, Byler S, Lapinska K, Willbanks A and Sarkar S: EMT and tumor metastasis. Clin Transl Oncol 4: 6, 2015.
27. Fujiki H, Sueoka E, Watanabe T and Suganuma M: Synergistic enhancement of anticancer effects on numerous human cancer cell lines treated with the combination of EGCG, other green tea catechins, and anticancer compounds. J Cancer Res Clin Oncol 141: 1511-1522, 2015.
28. Singh BN, Shankar S and Srivastava RK: Green tea catechin, epigallocatechin-3-gallate (EGCG): Mechanisms, perspectives and clinical applications. Biochem Pharmacol 82: 1807-1821, 2011.

29. Ramshankar V and Krishnamurthy A: Chemoprevention of oral cancer: Green tea experience. J Nat Sci Biol Med 5: 3-7, 2014.
30. Tao L, Park JY and Lambert JD: The differential pro-oxidative effects of the green tea polyphenol, (-)-epigallocatechin-3-gallate, in normal and oral cancer cells are related to differences in sirtuin 3 signaling. Mol Nutr Food Res 59: 203-211, 2015.
31. Martinez VD, Garnis C and Wan LL: Oral cancer. In: Encyclopedia of Cancer. Schwab M (ed). Springer, Berlin, pp3243-3245, 2017.
32. Schwam ZG and Judson BL: Improved prognosis for patients with oral cavity squamous cell carcinoma: Analysis of the National Cancer Database 1998-2006. Oral Oncol 52: 45-51, 2016.
33. Chen LL, Han WF, Geng Y and Su JS: A genome-wide study of DNA methylation modified by epigallocatechin-3-gallate in the CAL-27 cell line. Mol Med Rep 12: 5886-5890, 2015.
34. Hong JH, Hwang ES, Mcmanus MT, Amsterdam A, Tian Y, Kalmukova R, Mueller E, Benjamin T, Spiegelman BM, Sharp PA, et al: TAZ, a transcriptional modulator of mesenchymal stem cell differentiation. Science 309: 1074-1078, 2005.
35. Wei Z, Wang Y, Li Z, Yuan C, Zhang W, Wang D, Ye J, Jiang H, Wu Y and Cheng J: Overexpression of Hippo pathway effector TAZ in tongue squamous cell carcinoma: Correlation with clinicopathological features and patients' prognosis. J Oral Pathol Med 42: 747-754, 2013.
36. Liu C, Huang W and Lei Q: Regulation and function of the TAZ transcription co-activator. Int J Biochem Mol Biol 2: 247-256, 2011.
37. Ren QP, Fang YM, Zhu XH and Wang JX: Effects of EGCG on the proliferation and apoptosis of human oral squamous cell carcinoma Tca8113 cell line. J Oral Sci 28: 405-408, 2012 (In Chinese).
38. Sakagami H: Apoptosis-inducing activity and tumor-specificity of antitumor agents against oral squamous cell carcinoma. Jpn Dent Sci Rev 46: 173-187, 2010.
39. Hwang YS, Park KK and Chung WY: Epigallocatechin-3 gallate inhibits cancer invasion by repressing functional invadopodia formation in oral squamous cell carcinoma. Eur J Pharmacol 715: 286-295, 2013.
40. Meng Z, Moroishi T and Guan KL: Mechanisms of Hippo pathway regulation. Genes Dev 30: 1-17, 2016.
41. Meng Z, Moroishi T, Mottier-Pavie V, Plouffe SW, Hansen CG, Hong AW, Park HW, Mo JS, Lu W, Lu S, et al: MAP4K family kinases act in parallel to MST1/2 to activate LATS1/2 in the Hippo pathway. Nat Commun 6: 8357, 2015.
42. Champion A, Picaud A and Henry Y: Reassessing the MAP3K and MAP4K relationships. Trends Plant Sci 9: 123-129, 2004.
43. Sun G and Irvine KD: Ajuba family proteins link JNK to Hippo signaling. Sci Signal 6: ra81, 2013.
44. Wang SS, Chen YH, Chen N, Wang LJ, Chen DX, Weng HL, Dooley S and Ding HG: Hydrogen sulfide promotes autophagy of hepatocellular carcinoma cells through the PI3K/Akt/mTOR signaling pathway. Cell Death Dis 8: e2688, 2017.
45. Stine JE, Hui G, Sheng X, Han X, Schointuch MN, Gilliam TP, Gehrig PA, Zhou C and Bae-Jump VL: The HMG-CoA reductase inhibitor, simvastatin, exhibits anti-metastatic and anti-tumorigenic effects in ovarian cancer. Oncotarget 7: 946-960, 2016.